ADVANCED TURBULENCE MODELLING OF WINGTIP VORTICES

Alistair Revell
University of Manchester,
C42 George Begg Bdg., Manchester. UK.
alistair.revell@manchester.ac.uk

Karthikeyan Duraisamy
University of Glasgow,
623B James Watt Bdg., Glasgow. UK.
dkarthik@aero.gla.ac.uk

Gianluca Iaccarino
Stanford University,
500-I Stanford, CA. USA.
jops@stanford.edu

ABSTRACT

The performance of two 'modified' eddy viscosity models (EVM) is assessed in their application to trailing vortex flows. The curvature corrected $v^2 - f$ model Duraisamy and Iaccarino (2005) was specifically derived to account for the effects of rotation and streamline curvature, and is based on mimicking the behaviour of the equilibrium solution of Reynolds stress models (RSM) under homogeneous conditions. Focus is upon the Stress-Strain Lag (C_{as}) model, which was derived to capture the effects of misalignment between mean strain and turbulent stress fields, particularly for unsteady mean flows (Revell et al., 2006). In this work the model is coupled with the SST model to form the SST-C_{as} model, which is first validated for the case of an isolated Batchelor vortex.

Secondary to the main objective of the evaluation of EVMs, is to test an advanced unstructured meshing tool, which has the potential to offer huge economies in grid meshing. Both these goals serve a greater common purpose, which is the delivery of practical and economic alternatives to industrial users, where time and cost constraints are paramount.

Both modelling schemes are shown to respond correctly to the rotational effects of vortex flows, and the decay rates are well predicted. An unstructured mesh is used to compute the wingtip flow of Chow et al. (1997), employing $\sim 8\times$ less cells than that required for a grid independent solution on a structured mesh. While results are encouraging and considerable time economies are made, the same level of accuracy attained on the structured mesh is not reached, and further refinement and tuning is required.

INTRODUCTION

The numerical calculation of the vortex trailed from the wingtip of an aircraft has attracted significant attention in recent years. The vortex formation process over the wing surface involves cross-flow separation, and the evolving vortex suppresses turbulent mixing in the core. Accurate modelling of both of these phenomena is imperative in the successful prediction of trailing vortex flows. Evaluation of RANS closures for vortex evolution problems is further complicated by the fact that as a result of the stringent mesh requirements, it is usually difficult to separate numerical diffusion errors from turbulence modelling errors. For instance, the predictive capabilities of baseline turbulence models in Duraisamy and Iaccarino (2005) and Craft et al. (2006) are seen to vary largely, while the more complex or 'modified' turbulence models appear to improve performance in both studies.

Typical Reynolds numbers of trailing vortices flow make the application of Large Eddy Simulation (LES) approaches extremely challenging and computational intensive, and therefore simpler, more stable RANS models are favored. However, swirling flows - as with others characterized by strong streamline curvature - are notoriously difficult to model accurately within conventional, linear EVM closures.

The selected turbulence model must be capable of resolving the complex wing boundary layer as well as the swirling free shear flow downstream and as such it is perhaps unsurprising that relatively few CFD studies of this case have been reported. An early attempt by De Jong et al. (1988) at computing the vortex wake employing a simplified time-marching approach showed limited success. The first fully 3D fully-elliptic study of the vortex wake was made by Dacles-Mariani et al. (1995), who used a structured grid of 1.5×10^6 nodes and a basic one-equation model. In this more recent work the authors highlighted the need to modify the turbulence model to prevent excessive diffusion, which essentially corresponds to a curvature correction.

The experimental work of Chow et al. (1997) on this case has provided reference data for a number of recent numerical studies. In a European Union collaborative research project involving this test-case, it was seen that of a large selection of turbulence models, only the Reynolds stress models were consistently able to reproduce the correct axial-velocity overshoot (Haase *et al.* 2006). A range of numerical grids were used, and a strong grid sensitivity was clearly observed. The most accurate results were found when the largest grid (7.3×10^6 cells) was combined with the non-linear Reynolds stress-transport model of Craft et al. (1996a), the results of which are reported in the more detailed study of Craft et al. (2006).

A recent LES simulation of the same case was carried out by Uzun et al. (2006), who computed the flow at the lower Reynolds number of 0.5×10^6 in order to reduce the computational cost to an acceptable level. Despite this measure, a numerical grid of 26.2×10^6 nodes was required, and the authors report using 124 processors for between $23 - 57$ days dependent upon the processor speed. In addition, the reduction of Reynolds number is seen to have a significant effect on the predicted results. While the scale of this work is impressive it serves to underline the substantial costs associated with using LES for flows of this nature.

This paper first outlines the two main novel modelling schemes used, the curvature corrected $v^2 - f$ and the stress-strain lag model. The former has previously been validated in similar flow conditions, while the latter is validated here. Results are then presented for the

full wingtip calculation, where those performed on the unstructured grid form the majority of this work.

Modified $v^2 - f$ models

In order to account for frame-rotation effects, a modification was proposed to the $v^2 - f$ model by Pettersson-Reif et al. (1999). This is based on the behaviour of the equilibrium solution of homogeneous plane shear flow subject to orthogonal frame rotation. In essence, the eddy viscosity coefficient, C_μ, is replaced by $C^*_\mu(\eta_1, \eta_2)$, where

$$\eta_1 = T^2 \left|S_{ij}\right|^2 \quad and \quad \eta_2 = T^2 \left|\Omega_{ij} + C_\omega \epsilon_{jik}\omega_k\right|^2 \ , \quad (1)$$

T is the turbulent timescale, $C_\omega = 2.25$, ϵ_{jik} is the cyclic permutation tensor, ω_k is the angular frame velocity and the rates of strain and vorticity are defined as $S_{ij} = 1/2\left(\partial v_i/\partial x_j + \partial v_j/\partial x_i\right)$ and $\Omega_{ij} = 1/2\left(\partial v_i/\partial x_j - \partial v_j/\partial x_i\right)$ respectively. The final functional form was selected to be:

$$C^*_\mu(\eta_1, \eta_2) = C_\mu \frac{1 + \beta_2|\eta_3| + \beta_3|\eta_3|}{1 + \beta_4|\eta_3|} \left[\sqrt{\frac{1 + \beta_5\eta_1}{1 + \beta_5\eta_2}} + \beta_1\sqrt{\eta_2}\sqrt{|\eta_3| - \eta_3}\right]^{-1} \quad (2)$$

with $\eta_3 = \eta_1 - \eta_2$, which becomes zero in plane parallel shear in an intertial frame of reference. The model constants are given as $\{\beta_1, \beta_2, \beta_3, \beta_4, \beta_5\} = \{0.055, 0.5, 0.25, 0.2, 0.025\}$.

Curvature corrected $v^2 - f$. Curvature sensitivity can be introduced into an EARSM by transforming the anisotropy evolution equation to a *local* coordinate system in which the *weak* equilibrium condition can be approached. As shown in Gatski (2000) and Hellsten et al. (2002), curvature sensitivity can be incorporated by obtaining a Galilean invariant measure of the local rotation rate and including it in the objective vorticity tensor $\bar{\omega_k}$ in a consistent manner. A similar approach was proposed by Duraisamy and Iaccarino (2005) for the previously defined frame invariant $v^2 - f$ model, with the invariant η_2 now defined as:

$$\eta_2 = T^2 \left|\Omega ij + C_\omega \left(\epsilon_{jik}\omega_k - \epsilon_{ijk}\overline{\omega_k}\right)\right|^2 \ , \quad (3)$$

where $-\epsilon_{ijk}\overline{\omega}_k$ is an antisymmetric tensor that results from the transformation to a local basis, and is computed according to Wallin and Johansson (2002), as follows:

$$\bar{\omega}_i = \frac{\Pi_1^2\delta_{ij} + 12\Pi_2 S_{ij} + 6\Pi_1 S_{ik}S_{kj}}{2\Pi_1^3 - 12\Pi_2^2} S_{pl}S'_{lq}\epsilon_{pqj}, \quad (4)$$

where, $(.)'$ denotes a material derivative D/Dt, $\Pi_1 = trace\{S_{ij}^2\}$ and $\Pi_2 = trace\{S_{ij}^3\}$. In practice, the contribution of the curvature correction term is controlled.

The $v^2 - f$ model with curvature correction (CC) was applied to the Lamb-Oseen vortex; the simplified case of a homogenous line vortex (Duraisamy and Iaccarino, 2005). This analysis clearly indicated that the curvature correction reduces the effective eddy viscosity coefficient, C^*_μ and the increase in production to dissipation ratio with radius is much more gradual than both the standard and frame invariant versions of the $v^2 - f$ model.

The Stress-Strain Lag model

Inspired by work on cyclic piston engines by Hadžić et al. (2001), the Lag model builds upon existing two equation models with a third transport equation that is sensitive to the local stress-strain misalignment of mean unsteady turbulent flow (Revell, 2006). An early attempt to account for the stress-strain misalignment was proposed by Rotta (1979), who proposed a simplified tensorial eddy viscosity formulation to account for these effects in 3D thin-shear boundary layer flows. A more recent model, proposed by Olsen and Coakley (2001), couples a standard two equation model with a transport equation for the eddy viscosity, which enables relaxation effects to be captured, although it does not directly deal with the issue of misalignment.

The Lag model considered here defines the key parameter, C_{as}, representing the dot product of the strain tensor S_{ij}, and the turbulent stress anisotropy tensor a_{ij} as follows:

$$C_{as} = -\frac{a_{ij}S_{ij}}{\|S\|} \ , \quad (5)$$

where $a_{ij} = \overline{u_i u_j}/k - 2/3\delta_{ij}$ is the turbulence anisotropy tensor, $\overline{u_i u_j}$ is the Reynolds stress tensor, $k = 0.5\overline{u_i u_i}$ is the turbulent kinetic energy, δ_{ij} the Kronecker delta and the strain invariant $\|S\| = \sqrt{2S_{ij}S_{ij}}$.

The quantity C_{as} projects the six equations of the Reynolds stress transport model onto a single equation. The anisotropy tensor has zero trace and is dimensionless by definition, whereas the strain rate tensor is an inverse time scale and has zero trace only in the condition of incompressibility, which is assumed for this work. An EVM assumes that these two tensors are aligned.

The alignment for all quasi-2D flows is representable by a single dimensionless scalar. Three scalar values are necessary to define the stress-strain misalignment in a fully 3D flow, but in such cases, it is argued that some benefit will be gained from the scalar measure described above.

The strategy adopted for this scheme was to develop a transport equation that could be solved to obtain values for the parameter C_{as}. The resulting values could then be used in the evaluation of the production of turbulence kinetic energy P_k, in order to capture some of the features of stress-strain misalignment, but at a much smaller computational cost than employing a full stress transport model. For details on the derivation see Revell (2006). The final implemented form of the transport equation is given as follows:

$$\begin{aligned}\frac{DC_{as}}{Dt} &= \alpha_1\frac{\varepsilon}{k}C_{as} + \alpha_1^*\|S\|C_{as}^2 + \left(\alpha_3 + \alpha_3^*\sqrt{a_{ij}a_{ij}}\right)\|S\| \\ &+ \frac{S_{ij}a_{ik}}{\|S\|}\left(\alpha_4 S_{jk} + \alpha_5\Omega_{jk}\right) - \frac{S'_{ij}}{\|S\|}\left(a_{ij} + \frac{2S_{ij}C_{as}}{\|S\|}\right) \\ &+ \frac{\partial}{\partial x_k}\left[\left(\nu + \sigma_c\nu_t\right)\frac{\partial C_{as}}{\partial x_k}\right] \ , \end{aligned} \quad (6)$$

where ε is the rate of dissipation of turbulent kinetic energy and the model constants are given as $\{\alpha_1, \alpha_1^*, \alpha_3, \alpha_3^*, \alpha_4\,\alpha_5, \sigma_c\} = \{-0.7, -1.9, 0.267, 0.1625, 0.75, 1.6, 0.5\}$. Since Equation 6 is derived directly from an RSM, the constants of the selected pressure-strain model are retained and so in general, there is no requirement to calibrate these constants. It should be noted that when Equation 6 is coupled with the baseline $k - \omega$ SST model, it becomes necessary to use $\varepsilon = 0.09k\omega$ in order to obtain an appropriate value for ε.

The advection of the rate of strains in Equation 6 is calculated explicitly as follows, where the superscript n refers to the calculation timestep, the size of which is denoted as Δt:

$$S'_{ij} = \frac{S_{ij}^n - S_{ij}^{n-1}}{\Delta t} + U_k\frac{\partial S_{ij}^n}{\partial x_k} \ . \quad (7)$$

When computing gradients of S_{ij} on unstructured grids it sometimes becomes necessary to limit values, and this is done based upon neighbouring cells. Equation 6 is not in closed form as a model for a_{ij} is still required. This can be obtained from any existing NLEVM, and in the present work the model of Craft et al. (1996b) has been selected for this purpose.

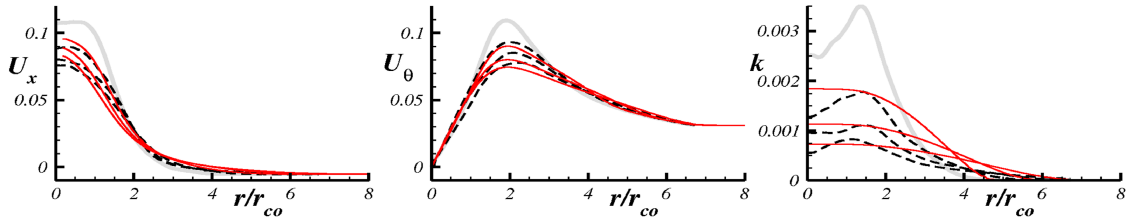

(a) RSM of Speziale et al. (1991)

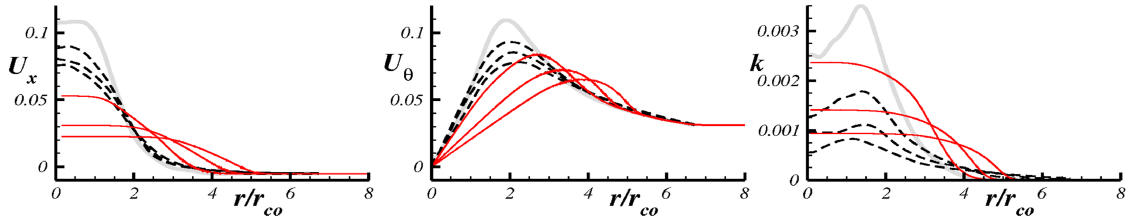

(b) Standard SST of Menter (1994)

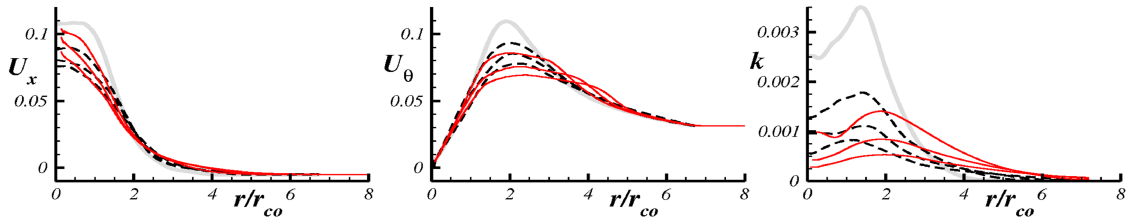

(c) The Lag model, SST-C_{as}

Figure 1: Evolution of mean axial velocity, U_x, tangential velocity, U_θ and turbulent kinetic energy k. RANS calculations initialised from DNS values at $t/T = 2.0$ (thick grey line). Results for $t/T = \{2.9, 4.8, 8.9\}$: – – – DNS; ——— RANS models.

The SST-C_{as} model. The fully implemented SST model requires only small modifications to incorporate the C_{as} model. The modification was originally intended to be applied to the production rate of turbulence kinetic energy term only, but it can be applied in a more coherent manner by means of a simple modification to the turbulent eddy viscosity as follows:

$$\nu_t = k\, min\left(\frac{1}{\omega}; \frac{0.31}{\|S\| F_2}; \frac{C_{as}}{\|S\|}\right) \tag{8}$$

where ω is the turbulent frequency and F_2 is a blending function which takes a value ≈ 1 across most of the boundary layer, dropping to 0 near the top and in the free-stream (see Menter, 1994, for details). The value of C_{as} in Equation 8 is limited to ± 0.31 for the calculation of the production terms, while when evaluating diffusion terms, the absolute value, $|C_{as}|$, is used. The current version requires special treatment in the near-wall region as a consequence of the modelling of the pressure-strain terms which are used in the derivation of Equation 6. For high Reynolds number flows of the kind considered in the present work, the simplest treatment consists of preventing the model from acting in regions where viscous effects are expected to be dominant.

Validation case: Isolated vortex. The Stress-Strain Lag model was derived primarily for mean unsteady flow applications, and has been shown to offer significant improvement in a variety of conditions (see Hoarau et al., 2005; Revell et al., 2006, 2007). Before attempting to compute the wingtip flow, the case of the temporal evolution of an isolated turbulent Batchelor vortex is investigated, since the idealised axisymmetric field is fairly representative of the mean flow field of practical trailing vortices.

Recently, Duraisamy and Lele (2006) performed Direct Numerical Simulation (DNS) of Batchelor vortex flows in order to gain a clearer understanding of the evolution of vortices which are normal mode unstable (i.e. swirl number, $q < 1.5$). They examined the complex evolution of helical instabilities, noting that these cases are characterised by a steep initial growth of the turbulent kinetic energy, followed by saturation and eventual decay. The initial base flow condition for tangential velocity, U_θ and axial velocity, U_x, are given by:

$$U_\theta = -\frac{U_o}{r\sqrt{\alpha}}\left(1 - e^{-\alpha r^2}\right), \; U_x = -\frac{U_o}{q} e^{-\alpha r^2}, \tag{9}$$

where $\alpha = 1.256$ so that the initial vortex core-radius is $r_{co} = 1$. Time is non-dimensionalised by the 'turnover time' $T = 2\pi U_0 / r_{co}$, and the Reynolds number (defined as $2\pi U_0/\sqrt{\alpha}/\nu$) is set to 8250 (corresponding to $q = 0.5$). They used a domain of width $15 r_{co}$ and a mesh size of 18.87×10^6 cells. It is beyond the ability and requirements of a turbulence model to correctly compute the complex interactions of the helical structures described by the DNS, and so the focus of this validation work is upon the decay phase of the vortex evolution. It is indeed the decay phase which dictates the performance of turbulence models in the wingtip vortex case, where cost constraints require the use of RANS.

The time evolution of an isolated vortex is calculated using a 2D circular grid of 8000 cells, with a spanwise extent of $20 r_{co}$. Several grid refinements were carried out to arrive at a grid-independent solution. Periodic boundary conditions were used in the axial flow direction and symmetry conditions were used in the directions normal to the axial flow.

Results are displayed in Figure 1 for the three RANS models: **a)** the SSG Reynolds stress model, **b)** the standard SST model and **c)** the SST-C_{as} model. In each case the calculations were initialised using DNS data from the results for $q = 0.5$ at $t/T = 2.0$, at which point the instabilities are seen to be saturated, and the mean flow is subsequently seen to revert back to equilibrium.

It is seen from Figure 1a that the Reynolds stress model does a

reasonable job of predicting the decay rate of both the axial and tangential velocity components. Predicted levels of $k = 0.5\overline{u_i u_i}$ are in reasonable agreement with the DNS, although there is no peak observed between $1 < r/r_{co} < 2$.

The predictions from the standard SST model in Figure 1b are considerably worse than the RSM, as the vortex is predicted to decay at a much greater rate. It is also seen from the plots of U_θ that the angular momentum spreads out further than indicated by the DNS, which is an indicator of excessive diffusion. In corroboration with this observation, the levels of turbulent kinetic energy predicted by the SST are higher than the DNS levels, which would lead to overpredictions of both production P_k and the turbulent diffusion. Despite being overpredicted, the levels of k returned by the SST model are closer to DNS values by accident; as a consequence of the erroneous flattening of the U_x profiles, since if the correct profile were forced, larger gradients would generate even higher values of k via the production term.

The results returned from the SST-C_{as} model shown in Figure 1c are broadly in agreement with the RSM predictions, although the level of turbulence at the vortex core is seen to fall lower than it should. This explains why the axial velocity at the vortex centre itself are higher than the DNS values. In general, it appears that an improved modelling of P_k via the influence of the C_{as} term leads to a more accurate prediction of the levels of k and thus the mean velocities.

WINGTIP CASE SETUP

The experiment conducted by Chow et al. (1997) corresponds to a rounded tip NACA 0012 wing of 4 ft. chord and 3 ft. span in a $32 \times 48in.$ wind tunnel section. The chord based Reynolds number is 4.35×10^6 and the angle of attack is 10^o. The flow is tripped at the leading edge so that the flow can be considered fully turbulent.

The structured grid. A multiblock structured grid consisting of 9.3×10^6 mesh points and 62 blocks was used for the computation. A sample streamwise section of the grid is shown in Figure 3a. As seen in the figure, the mesh points are very finely clustered in the region of vortex formation. All computations on this grid were performed using the Stanford Multi-Block structured mesh solver SUmB, which is a scalable compressible RANS code (van der Weide et al., 2005). Calculations were run using a third order accurate convection scheme and results were computed for each of the three different $v^2 - f$ based models, described above.

The unstructured grid. The unstructured grid was created using an *in-house* mesh-generator and for the calculations presented here, the grid contained around $\approx 1.2 \times 10^6$ cells; almost a factor of 10 less than the structured grid, (see Figure 3b). The approximate path of the trailing vortex was extracted from a precursor calculation and used to build the present mesh, with particular attention paid to the regions around the wingtip and the wing leading-edge.

Calculations on the unstructured grid were performed using *Code_Saturne*, an unstructured finite-volume code from *EDF*, which uses a collocated discretisation for cells of any shape (Archambeau et al., 2004). It solves turbulent Navier-Stokes equations for Newtonian incompressible flows with a fractional step method based on a prediction-correction algorithm for pressure/velocity coupling (SIMPLEC) and a momentum interpolation to avoid pressure oscillations.

Transition was tripped at $x/c = 0.04$ for the SST based calculations, while the high Reynolds number version of the RSM (SSG) was used with a standard wall function treatment. The SST model was computed first and its results were used to initialise the RSM and SST-C_{as} calculations. In order to assist convergence, the values of S'_{ij} were limited in the SST-C_{as} model calculations.

RESULTS

Figure 5 shows the normalised turbulent viscosity contours, ν_t/ν, at a downstream location of $x/c = 0.246$ (the trailing edge is at $x/c = 0$). The modified $v^2 - f$ (CC) and SST-C_{as} models are compared to their respective baseline models, which are shown to predict maximum levels of ν_t/ν near centre of the vortex core, which is unphysical in light of the stabilising effects of solid body rotation. Both modified models predict much lower values of turbulent viscosity in the vortex core region, which corresponds to lower levels of turbulence kinetic energy and thus a slower decay of the trailing vortex. The results on unstructured grid, from the standard SST and the SST-C_{as}, display larger values of ν_t/ν in the wake region of the wing. This is a due to the very large cell sizes in this region and the subsequent poor resolution of the flow. The fact that the standard SST model reports low levels of turbulent viscosity in the centre of the vortex core is somewhat surprising since the model has no inherent ability to account for frame rotation effects, however this could be due to the viscosity limiter in the model. It is possible that an unphysical flow feature is being introduced into the calculation as an adverse effect of the unstructured mesh and so further refinement studies are required to investigate this.

Figure 4 shows the axial component of velocity along a horizontal line passing through the core of vortex at $x/c = 0.456$. Figure 4a shows the results from the different variants of the $v^2 - f$ models on the structured grid. A small improvement over the baseline model is reported from the frame-rotation version, which at least predicts a peak of axial velocity in the correct region. Clearly, the inclusion of the Curvature Correction drastically improves the prediction, returning a value of $U_x \sim 1.65$ compared to an experimental value of $U_x \sim 1.75$. Accurate computation of the axial velocity is critical to the correct prediction of the swirl velocity because of the radial transport of angular momentum that is associated with the presence of strong gradients of axial velocity.

Figure 4b reports corresponding results from the RSM, the SST and the SST-C_{as} model on the unstructured mesh. As expected, the full Reynolds stress model returns the highest value of U_x, reaching a peak value of ~ 1.52, while the standard SST model performs poorly. The SST-C_{as} model predicts a peak value of $U_x \sim 1.41$ which is a substantial improvement over the baseline model.

Figure 6 shows a comparison of mean flow quantities at a location of $x/c = 0.456$ downstream of the trailing edge. While the peak axial velocities, U_x, have already been compared in Figure 4, more information about the mean flow structure can be ascertained from Figures 6a and 6b. From the contours of tangential velocity, the numerical predictions from both the RSM and the SST-C_{as} predict two peak values either side of the vortex core, while the experiment reveals only one. In addition, the gradients of tangential velocity near the vortex core are lower in the numerical results than in the experiment, indicating excessive diffusion of angular momentum. Further work is required to ascertain the extent of detrimental grid-induced flow features.

In Figure 6c, it can be seen that the levels of turbulence kinetic energy, predicted by both the RSM and the SST-C_{as} model are far lower than indicated in the experiment, while those from the standard SST are larger. Erroneously low levels of C_{as} may well be responsible for this reduction in turbulence, although similar findings were reported in the work by Craft et al. (2006) for RSM predictions, and the source of this problem remains unclear.

CONCLUSIONS

This study has reported the performance of two modified turbulence models in predicting the development of trailing vortices. In general, the models are seen to be sensitive to the effects of flow rotation via the reduction of ν_t and thus the production of k. Levels of U_x are well predicted downstream of the trailing edge, but levels of

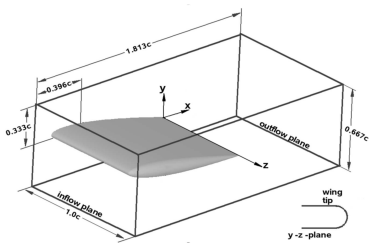

Figure 2: Layout of Wingtip Expt.

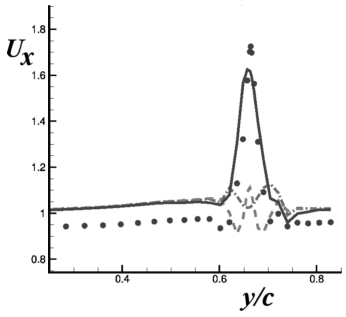

(a) Results from structured grid. Expt. (•); Standard $v^2 - f$ (— · —) ; Frame rotation $v^2 - f$ (– – –); Curvature Corrected $v^2 - f$ (————)

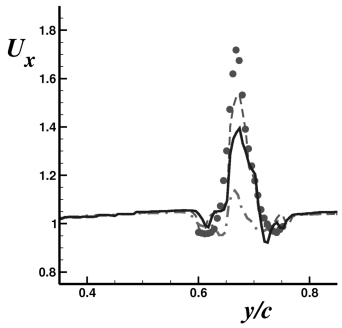

(b) Results from unstructured grid. Expt. (•); Standard SST (— · —) ; RSM (– – –); Lag model, SST-C_{as} (————)

Figure 4: Axial velocity, U_x, along a line passing through the vortex core at $x/c = 0.456$, for a selection of different RANS models on both the structured and unstructured grids.

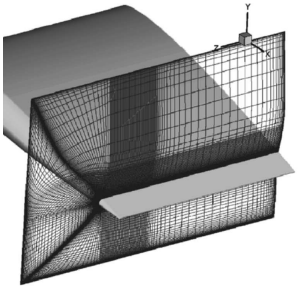

(a) YZ plane in structured grid of 9.3×10^6 cells

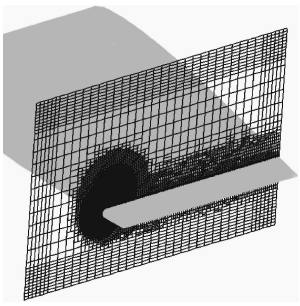

(b) YZ plane in unstructured grid of 1.2×10^6 cells

Figure 3: Comparison of the Grids used in the wingtip calculations.

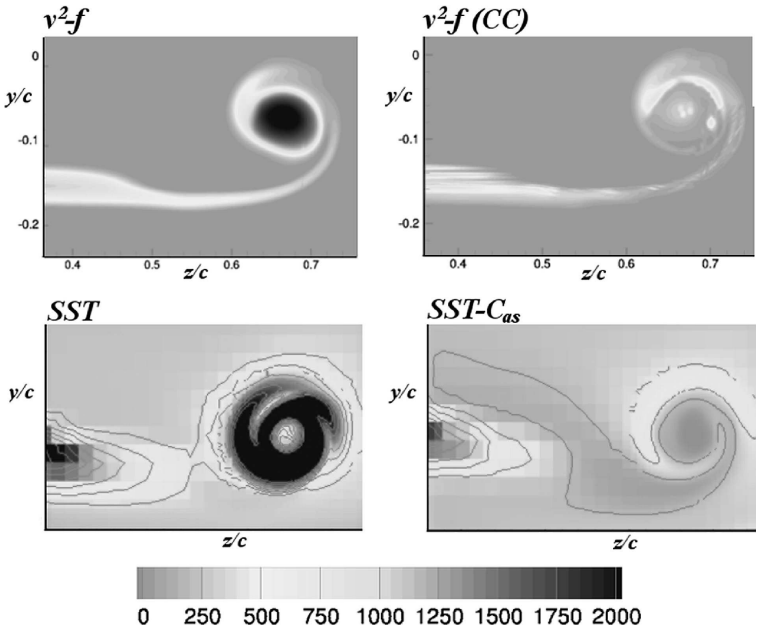

Figure 5: Contours of normalised turbulent viscosity, ν_t/ν, at $x/c = 0.246$; modified models compared to baseline models.

k are seen to drop away too drastically. Further work is required to improve the predictive capabilities of these models to return a more accurate turbulence decay rate.

Results for the curvature corrected $v^2 - f$ on the structured mesh are very encouraging and yielded drastic improvements over the baseline $v^2 - f$ model. Solutions from the unstructured mesh were not in quite as good an agreement with experimental values, but may well improve with further mesh refinement, whilst maintaining significant economies.

The abrupt transition from small to large cell volumes can lead to numerical errors, or unphysical flow features. To avoid this, one either has to ensure a more gradual cell volume transition, thus necessitating more cells and offsetting economic benefit, or alternatively, one has to be certain that numerical errors arising from coarse cells do not adversely effect the rest of the domain. In this work, the resolution of the wake downstream of the trailing edge is seen to be under-resolved and could be a potential source of error.

The main advantage of structured meshes lies in the ability to employ high-order-accurate numerical schemes, which is currently not an option within most unstructured codes. Further work is required to assess the limit to which the current unstructured solutions can be improved by mesh refinement alone. Regardless, this study helps to demonstrate that unstructured meshing has a lot of potential to bring more complex calculations closer into the practical reach of everyday CFD useage, particularly for industry.

Acknowledgements. Support from CTR during the Summer Program 2006 is gratefully acknowledged. AR would also like to thank T. Craft and D. Laurence for discussions about modelling issues. This work was partially supported by the DESider Project, funded by the European Community in the 6th Framework Programme, under contract No. AST3-CT-2003-502842.

REFERENCES

Archambeau, F., Mechitoua, N., Sakiz, M., 2004. A finite volume method for the computation of turbulent incompressible flows - industrial applications. Int. J. Finite Volumes 1, 1–62.

Chow, J. S., Zilliac, G., Bradshaw, P., 1997. Turbulence measurements in the near field of a wingtip vortex. Tech. Rep. Tech Mem 110418, NASA.

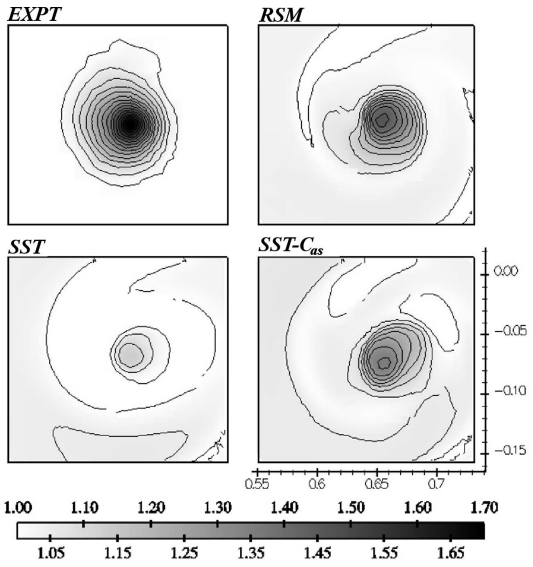

(a) Contours of axial velocity, U_x;

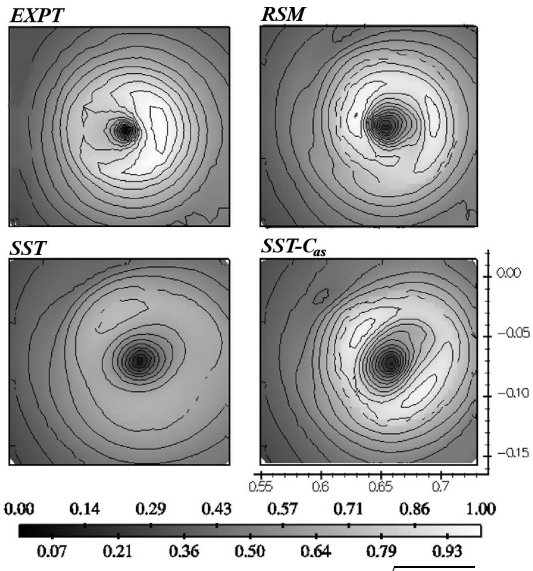

(b) Contours of tangential velocity, $U_\theta = \sqrt{U_y^2 + U_z^2}$;

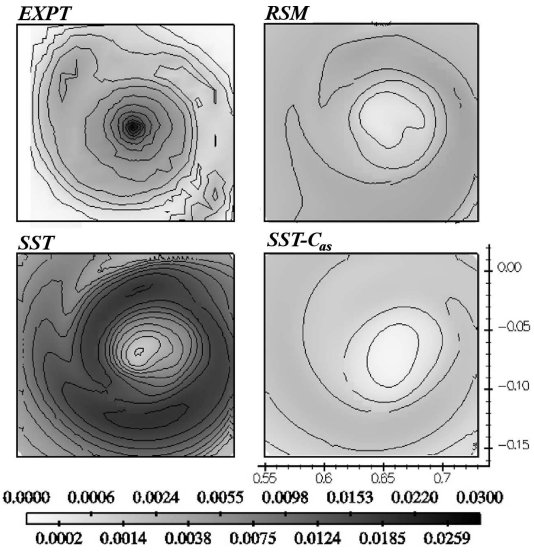

(c) Contours of turbulent kinetic energy, k;

Figure 6: Predicted mean flow quantities at $x/c = 0.456$ on the unstructured grid. 15 contours at regular linear intervals, except for k where the intervals grow quadratically.

Craft, T. J., Gerasimov, A. V., Launder, B. E., Robinson, C. M. E., 2006. A computational study of the near-field generation and decay of wingtip vortices. Int. J. Heat Fluid Flow 27, 684–695.

Craft, T. J., Ince, N. Z., Launder, B. E., 1996a. Recent developments in second-moment closure for buoyancy affected flows. Dynamics of Atmospheres and Oceans 23, 99–114.

Craft, T. J., Launder, B. E., Suga, K., 1996b. Development and application of cubic eddy-viscosity model of turbulence. Int. J. Heat Fluid Flow 17, 108–115.

Dacles-Mariani, J., Zilliac, G., S., C. J., Bradshaw, P., 1995. Numerical/experimental study of a wingtip vortex in the near field. AIAA J. 33 (9), 1561–1568.

De Jong, F. J., Govindan, T. R., Levy, R., Shamroth, S. J., 1988. Validation of a forward marching proceedure to compute tip vortex generation processes for ship propeller blades. Tech. Rep. Report R88-920023, Scientific Research Associates Inc.

Duraisamy, K., Iaccarino, G., 2005. Curvature correction and application of the $v^2 - f$ turbulence model to tip vortex flows. In: CTR. Annual Research Briefs 2005. Stanford, pp. 157–168.

Duraisamy, K., Lele, S. K., 2006. Dns of temporal evolution of isolated turbulent vortices. In: CTR. Proc. Summer Program 2006. Stanford, US., pp. 35–47.

Gatski, T. B. Jongen, T., 2000. Nonlinear eddy viscosity and algebraic stress models for solving complex turbulent flows. Progress in Aerospace Sciences 36, 655–682.

Hadžić, I., Hanjalić, K., Laurence, D., 2001. Modeling the response of turbulence subjected to cyclic irrotational strain. Phys. fluids 13 (6), 1740–1747.

Hellsten, A., Wallin, S., Laine, S., 2002. Scrutinizing curvature corrections for algebraic reynolds stress models. AIAA-paper, 2002-2963.

Hoarau, Y., Revell, A. J., Braza, M., Laurence, D., Barthet, A., 2005. Physical analysis and modelling of turbulent unsteady flows around a wing. In: Proc. Int. Symp. Bluff Body Wakes and Vortex Induced Vibrations-4. Santorini, Greece.

Menter, F. R., 1994. Two-equation eddy-viscosity turbulence models for engineering applications. AIAA J. 32, 1598–1605.

Olsen, M. E., Coakley, T. J., 2001. The lag model, a turbulence model for non equilibrium flows. AIAA paper,2001-2564.

Pettersson-Reif, B. A., Durbin, P. A., Ooi, A., 1999. Modeling rotational effects in eddy-viscosity closures. Int. J. Heat Fluid Flow 20, 563–573.

Revell, A. J., 2006. A stress - strain lag eddy viscosity model for mean unsteady turbulent flows. Ph.D. thesis, Dept. of Mech., Aero. & Civ. Eng., The University of Manchester.

Revell, A. J., Benhamadouche, S., Craft, T., Laurence, D., 2006. A stressstrain lag eddy viscosity model for unsteady mean flow. Int. J. Heat Fluid Flow 27, 821–830.

Revell, A. J., Craft, T., Laurence, D., 2007. Turbulence modelling of strongly detached unsteady flows: the circular cylinder. In: 2nd Symp. on Hybrid RANS-LES Methods. Springer.

Rotta, J. C., 1979. A family of turbulence models for three-dimensional thin shear layers. In: Durst, F. e. a. (Ed.), Turbulent Shear Flows 1. Springer-Verlag, Berlin, pp. 267–278.

Speziale, C. G., Sarkar, S., Gatski, T. B., 1991. Modeling the pressure strain correlation of turbulence: an invariant dynamical systems approach. J. Fluid Mech. 227, 245–272.

Uzun, A., Hussaini, M. Y., Streett, C. L., 2006. Large-eddy simulation of a wingtip vortex on overset grids. AIAA J. 44 (6), 1229–1242.

van der Weide, E., Kalitzin, G., Schulter, J., Medic, G., Alonso, J., 2005. On large scale turbomachinery computations. In: CTR. Annual Research Briefs 2005. Stanford, pp. 139–150.

Wallin, S., Johansson, A. V., 2002. Modelling streamline curvature effects in explicit algebraic stress turbulence models. Int. J. Heat Fluid Flow 23, 721–730.